Weierstraß-Institut

für Angewandte Analysis und Stochastik

Leibniz-Institut im Forschungsverbund Berlin e. V.

Preprint ISSN 2198-5855

Numerical studies of higher order variational time stepping schemes for evolutionary Navier–Stokes equations

Naveed Ahmed[1], Gunar Matthies[2]

submitted: October 27, 2016

[1] Weierstraß-Institut
Mohrenstr. 39
10117 Berlin
Germany
email: naveed.ahmed@wias-berlin.de

[2] Technische Universität Dresden
Institut für Numerische Mathematik
01062 Dresden
Germany
email: gunar.matthies@tu-dresden.de

No. 2322
Berlin 2016

2010 *Mathematics Subject Classification.* 76D05, 65M20, 65M60.

Key words and phrases. ransient incompressible Navier–Stokes equations, inf-sup stable pairs of finite element spaces, discontinuous Galerkin methods, continuous Galerkin–Petrov methods.

Edited by
Weierstraß-Institut für Angewandte Analysis und Stochastik (WIAS)
Leibniz-Institut im Forschungsverbund Berlin e. V.
Mohrenstraße 39
10117 Berlin
Germany

Fax: +49 30 20372-303
E-Mail: preprint@wias-berlin.de
World Wide Web: http://www.wias-berlin.de/

Abstract We present in this paper numerical studies of higher order variational time stepping schemes combined with finite element methods for simulations of the evolutionary Navier-Stokes equations. In particular, conforming inf-sup stable pairs of finite element spaces for approximating velocity and pressure are used as spatial discretization while continuous Galerkin–Petrov methods (cGP) and discontinuous Galerkin (dG) methods are applied as higher order variational time discretizations. Numerical results for the well-known problem of incompressible flows around a circle will be presented.

1 Introduction

The flow of incompressible fluids is described by the time-dependent, incompressible Navier–Stokes equations. In order to solve them numerically, one has to discretize in space and time. Often the method of lines is applied where the problem is discretized in space first while the time remains continuous. This technique leads to a large system of ordinary differential equations which can be solved by suitable ODE solvers. Note that the resulting system of ODE is nonlinear due to the nonlinear convection term in the Navier–Stokes equations.

We will consider continuous Galerkin–Petrov and discontinuous Galerkin methods as higher order variational time discretizations. In continuous Galerkin–Petrov (cGP) methods, the ansatz functions are continuous in time while the discontinuous test functions allow a time marching process. In discontinuous Galerkin (dG) schemes, ansatz and test functions are from the space and allowed to be discontinuous at the discrete time points. Hence, a time marching process is possible as well. The cGP method has been studied in [1] for the heat equation. Theoretical and numerical investigations of higher order variational time discretizations applied to different type of incompressible flow problems can be found in [2–6]. Note that cGP methods are A-stable whereas dG methods are even strongly A-stable which might lead to different damping properties with respect to high frequency error components. We refer to [7] for more information on dG methods.

The inf-sup condition plays a fundamental role for solving incompressible flow problems without additional pressure stabilization. Using inf-sup stable pairs of finite element space for approximation velocity and pressure is guided by the observation that flow problems are often part of coupled problems of flow and transport where mass conservation depends crucially on the properties of the discrete velocity, see [8]. Since the property of a velocity field being discretely divergence-free is disturbed by pressure stabilization, the use of inf-sup stable discretizations is favorable.

We will describe in this paper the discretization of the evolutionary Navier–Stokes equations in space by inf-sup stable finite element pairs for approximating velocity and pressure together with higher order

variational time stepping schemes using continuous Galerkin–Petrov and discontinuous Galerkin methods. In addition, a post-processing technique given in [9] for systems of ordinary differential equations is adapted in order to improve the accuracy of the numerical solution. The proposed solution strategy will be applied to the well-know benchmark problem of an incompressible flow around a circle.

The remainder of this paper is organized as follows. Section 2 introduces the evolutionary, incompressible Navier–Stokes equations and their finite element discretizations. Variational time discretizations by continuous Galerkin–Petrov and discontinuous Galerkin methods are described in Section 3 where also the post-processing techniques is given. Numerical results for the benchmark problem "flow around a circle" will be given in Section 4.

2 Model problem and its finite element discretization

Let $\Omega \subset \mathbb{R}^d$, $d \in \{2,3\}$, be a Lipschitz domain with polyhedral boundary $\partial\Omega$ and $T > 0$ a finite time. The motion of incompressible fluids is modeled by the time-dependent, incompressible Navier–Stokes equations which in dimensionless form are defined by

$$\begin{aligned} \mathbf{u}' - \nu\Delta\mathbf{u} + (\mathbf{u}\cdot\nabla)\mathbf{u} + \nabla p = \mathbf{f} \qquad & \text{in } (0,T]\times\Omega, \\ \nabla\cdot\mathbf{u} = 0 \qquad & \text{in } (0,T]\times\Omega. \end{aligned} \tag{1}$$

Here, $\mathbf{f}$ is a given body force, ν the viscosity, $\mathbf{u}$ and p denote the velocity and pressure fields, respectively. The partial differential equations in (1) have to be closed by appropriate initial and boundary conditions. For simplicity, we consider homogeneous Dirichlet boundary conditions on $[0,T]\times\partial\Omega$ and a given initial velocity field $\mathbf{u}_0$ in Ω.

We introduce the spaces $\mathbf{V} = H_0^1(\Omega)^d$, $Q = L_0^2(\Omega)$, and $W = \{\mathbf{v} \in L^2(0,T;\mathbf{V}) : \mathbf{v}' \in L^2(0,T;\mathbf{V}')\}$ with $\mathbf{V}' = H^{-1}(\Omega)^d$ as dual space of $\mathbf{V}$.

Assuming $\mathbf{f} \in L^2\big(0,T;L^2(\Omega)^d\big)$, a variational formulation of problem (1) reads:

Find $\mathbf{u} \in W$ and $p \in L^2(0,T;Q)$ such that $\mathbf{u}(0) = \mathbf{u}_0$ and for almost all $t \in (0,T)$

$$\begin{aligned} \langle \mathbf{u}'(t), \mathbf{v}\rangle + \nu(\nabla\mathbf{u}(t), \nabla\mathbf{v}) + ((\mathbf{u}(t)\cdot\nabla)\mathbf{u}(t), \mathbf{v}) - (p(t), \nabla\cdot\mathbf{v}) = (\mathbf{f}(t), \mathbf{v}) \qquad & \forall \mathbf{v} \in \mathbf{V}, \\ (q, \operatorname{div}\mathbf{u}) = 0 \qquad & \forall q \in Q. \end{aligned} \tag{2}$$

Note that $\langle\cdot,\cdot\rangle$ denote the duality pairing between $\mathbf{V}$ and $\mathbf{V}'$ while $(\cdot,\cdot)$ is the inner product in $L^2(\Omega)$ and its vector-valued and tensor-valued versions. The corresponding L^2-norm is given by $\|\cdot\|_0$ while $|\cdot|_m$ indicates the semi-norm in $H^m(\Omega)$ and its vector-valued version.

For finite element discretizations of (2), we are given a family $\{\mathscr{T}_h\}$ of shape-regular decomposition of Ω into d-simplices, quadrilaterals, or hexahedra. The diameter of a cell K is denoted by h_K and the mesh size h is defined by $h := \max_{K\in\mathscr{T}_h} h_K$.

We consider pairs of conforming finite element spaces $\mathbf{V}_h \subset \mathbf{V}$ and $Q_h \subset Q$ for approximation velocity and pressure where we assume that $\mathbf{V}_h = Y_h^d$ with a scalar finite element space Y_h. The unique solvability of the system arising from the discretization and linearization of (2) in space requires to satisfy the inf-sup stability condition

$$\inf_{q_h\in Q_h}\sup_{\mathbf{v}_h\in\mathbf{V}_h} \frac{(q_h, \nabla\cdot\mathbf{v}_h)}{\|q_h\|_0 |\mathbf{v}_h|_{1,h}} \geq \beta > 0. \tag{3}$$

Then, the finite element discretization of (2) reads:

Find $\mathbf{u}_h \in H^1(0,T;\mathbf{V}_h)$ and $p_h \in L^2(0,T;Q_h)$ such that with $\mathbf{u}_h(0) = \mathbf{u}_{0,h}$ and for almost all $t \in (0,T)$

$$(\mathbf{u}_h'(t), \mathbf{v}_h) + A\left(\mathbf{u}_h(t), (\mathbf{u}_h(t), p_h(t)), (\mathbf{v}_h, q_h)\right) = (\mathbf{f}(t), \mathbf{v}_h) \quad \forall (\mathbf{v}_h, q_h) \in \mathbf{V}_h \times Q_h \tag{4}$$

where $\mathbf{u}_{0,h} \in \mathbf{V}_h$ is a suitable approximation of the initial velocity $\mathbf{u}_0$ and A is defined by

$$A\left(\mathbf{w}, (\mathbf{u}, p), (\mathbf{v}, q)\right) = \nu(\nabla\mathbf{u}, \nabla\mathbf{v}) + ((\mathbf{w}\cdot\nabla)\mathbf{u}, \mathbf{v}) - (p, \nabla\cdot\mathbf{v}) + (q, \nabla\cdot\mathbf{u})$$

Note that A is linear in its second and third argument while the problem (4) is nonlinear.

3 Variational time-stepping schemes

In this section, we discretize problem (4) in time by continuous Galerkin–Petrov (cGP) and discontinuous Galerkin (dG) methods. To this end, we consider a partition $0 = t_0 < t_1 < \ldots < t_N = T$ of the time interval $I := [0,T]$ and set $I_n := (t_{n-1}, t_n]$, $\tau_n = t_n - t_{n-1}$, $n = 1,\ldots,N$, and $\tau := \max_{1\le n\le N} \tau_n$. For a given non-negative integer k, we define the time-continuous and time-discontinuous velocity spaces

$$X_k^{\mathrm{c}} := \Big\{ \mathbf{u} \in C(0,T;\mathbf{V}_h) : \mathbf{u}|_{I_n} \in \mathbb{P}_k(I_n,\mathbf{V}_h), n = 1,\ldots,N \Big\},$$
$$X_k^{\mathrm{dc}} := \Big\{ \mathbf{u} \in L^2(0,T;\mathbf{V}_h) : \mathbf{u}|_{I_n} \in \mathbb{P}_k(I_n,\mathbf{V}_h), n = 1,\ldots,N \Big\}$$

and time-continuous and time-discontinuous pressure spaces

$$Y_k^{\mathrm{c}} := \Big\{ q \in C(0,T;Q_h) : q|_{I_n} \in \mathbb{P}_k(I_n,Q_h), n = 1,\ldots,N \Big\},$$
$$Y_k^{\mathrm{dc}} := \Big\{ q \in L^2(0,T;Q_h) : q|_{I_n} \in \mathbb{P}_k(I_n,Q_h), n = 1,\ldots,N \Big\}$$

where

$$\mathbb{P}_k(I_n,W_h) := \Big\{ u : I_n \to W_h : u(t) = \sum_{i=0}^{k} U_i t^i, t \in I_n, U_i \in W_h, i = 0,\ldots,k \Big\}$$

denotes the space of W_h-valued polynomials of degree less than or equal to k in time. The function in the spaces X_k^{dc} and Y_k^{dc} are allowed to be discontinuous at the nodes t_n, $n = 1,\ldots,N-1$. For a piecewise smooth function w, let

$$w_n^- := \lim_{t\to t_n - 0} w(t), \quad w_n^+ := \lim_{t\to t_n + 0} w(t), \quad [w]_n := w_n^+ - w_n^-$$

denote the left-sided value, the right-sided value, and the jump, respectively.

3.1 The continuous Galerkin-Petrov method

In this section, we discretize the semi-discrete problem (4) in time by cGP methods to obtain a fully discrete formulation of (2). Now, the cGP(k) method reads:

Find $\mathbf{u}_{h,\tau} \in X_k^{\mathrm{c}}$ and $p_{h,\tau} \in Y_k^{\mathrm{c}}$ such that $\mathbf{u}_h(0) = \mathbf{u}_{0,h}$ and

$$\int_0^T \left[(\mathbf{u}'_{h,\tau}, \mathbf{v}_{h,\tau}) + A\left(\mathbf{u}_{h,\tau}, (\mathbf{u}_{h,\tau}, p_{h,\tau}), (\mathbf{v}_{h,\tau}, q_{h,\tau})\right) \right] = \int_0^T (\mathbf{f}, \mathbf{v}_{h,\tau}) \qquad \forall \mathbf{v}_{h,\tau} \in X_{k-1}^{\mathrm{dc}}, \forall q_{h,\tau} \in Y_{k-1}^{\mathrm{dc}} \tag{5}$$

where the index h,τ refers to the full discretization in space and time, respectively.

Since the test functions are allowed to be discontinuous at the discrete time points t_n, $n = 1,\ldots,N-1$, we can choose the test function $(\mathbf{v}_{h,\tau}, q_{h,\tau}) = (\mathbf{v}_h, q_h)\psi(t)$ with time independent $(\mathbf{v}_h, q_h) \in \mathbf{V}_h \times Q_h$ and a scalar function $\psi : I_n \to \mathbb{R}$ which is zero on $I \setminus I_n$ and a polynomial of degree less than or equal to $k-1$ on I_n. Then, the solution of the cGP(k) method can be determined by successively solving a single local problem on each time interval.

The fully discrete time marching scheme associated to (5) reads:

Find $\mathbf{u}_{h,\tau}\big|_{I_n} \in \mathbb{P}_k(I_n,\mathbf{V}_h)$ and $p_{h,\tau}\big|_{I_n} \in \mathbb{P}_k(I_n,Q_h)$ such that for all $\psi \in \mathbb{P}_{k-1}(I_n)$

$$\int_{I_n} \left[(\mathbf{u}'_{h,\tau}, \mathbf{v}_h) + A\left(\mathbf{u}_{h,\tau}, (\mathbf{u}_{h,\tau}, p_{h,\tau}), (\mathbf{v}_h, q_h)\right) \right] \psi(t) = \int_0^T (\mathbf{f}, \mathbf{v}_h)\psi(t) \qquad \forall (\mathbf{v}_h, q_h) \in \mathbf{V}_h \times Q_h$$

with $\mathbf{u}_{h,\tau}\big|_{I_1}(t_0) = \mathbf{u}_{0,h}$ and $\mathbf{u}_{h,\tau}\big|_{I_n}(t_{n-1}) = \mathbf{u}_{h,\tau}\big|_{I_{n-1}}(t_{n-1})$ for $n \ge 2$.

We apply for the numerical integration of the time integrals the Gauß-Lobatto quadrature rule with $(k+1)$ points. This formula is exact for polynomials of degree less than or equal to $2k-1$. Let $\hat{t}_j$ and $\hat{w}_j$, $j = 0,\ldots,k$, be the Gauß-Lobatto points and the corresponding quadrature weights on $[-1,1]$, respectively. Furthermore,

we denote by $\hat{\phi}_j \in \mathbb{P}_k$, $j = 0,\dots,k$, and $\hat{\psi}_j \in \mathbb{P}_{k-1}$, $j = 1,\dots,k$, the Lagrange basis function with respect to $\hat{t}_j$, $j = 0,\dots,k$, and $\hat{t}_j$, $j = 1,\dots,k$, respectively. The time polynomials $\phi_{n,j} \in \mathbb{P}_k(I_n)$, $j = 0,\dots,k$, and $\psi_{n,j} \in \mathbb{P}_{k-1}(I_n)$, $j = 1,\dots,k$, are defined by

$$\phi_{n,j}(t) := \hat{\phi}_j\left(T_n^{-1}(t)\right) \quad \text{and} \quad \psi_{n,j}(t) := \hat{\psi}_j\left(T_n^{-1}(t)\right)$$

with the affine reference transformation

$$T_n : [-1,1] \to \overline{I_n}, \quad \hat{t} \mapsto t_{n-1} + \frac{\tau_n}{2}(\hat{t}+1), \tag{6}$$

see [9].

Since the restrictions of $\mathbf{u}_{h,\tau}$ and $p_{h,\tau}$ to the interval I_n are $\mathbf{V}_h$-valued and Q_h-valued polynomials of degree less than or equal to k , they can be represented as

$$\mathbf{u}_{h,\tau}\big|_{I_n} = \sum_{j=0}^{k} U_{n,h}^j \phi_{n,h}^j(t), \quad p_{h,\tau}\big|_{I_n} = \sum_{j=0}^{k} P_{n,h}^j \phi_{n,h}^j(t), \quad t \in I_n,$$

with coefficients $U_{n,h}^j \in \mathbf{V}_h$ and $P_{n,h}^j \in Q_h$, $j = 0,\dots,k$. The particular ansatz ensures

$$\mathbf{u}_{h,\tau}(t_{n,j}) = U_{n,h}^j, \quad p_{h,\tau}(t_{n,j}) = P_{n,h}^j, \quad j = 0,\dots,k,$$

where $t_{n,j} := T_n(\hat{t}_j)$, $j = 0,\dots,k$. Since $t_{n,0} = t_{n-1}$ and $t_{n,k} = t_n$ hold, the initial conditions on the intervals I_n, $n = 1,\dots,N$, are equivalent to the conditions

$$U_{1,h}^0 = \mathbf{u}_{0,h}, \quad \text{and} \quad U_{n,h}^0 = \mathbf{u}_{h,\tau}\big|_{I_n}(t_{n-1}) = U_{n-1,h}^k \quad \text{if } n \geq 2.$$

Using the properties of the basis functions in time, we obtain the following coupled system of nonlinear equations:

For $U_{1,h}^0 = \mathbf{u}_{0,h}$ and $U_{n,h}^0 = U_{n-1,h}^k$ if $n \geq 2$, find the coefficients $U_{n,h}^j \in \mathbf{V}_h$ and $P_{n,h}^j$, $j = 1,\dots,k$, such that

$$\sum_{j=0}^{k} \alpha_{i,j}^c \left(U_{n,h}^j, \mathbf{v}_h\right) + \frac{\tau_n}{2} A\left(U_{n,h}^i, (U_{n,h}^i, P_{n,h}^i), (\mathbf{v}_h, q_h)\right) = \frac{\tau_n}{2}\left\{ (\mathbf{f}(t_{n,i}), \mathbf{v}_h) + \beta_i^c \left(\mathbf{f}(t_{n-1}), \mathbf{v}_h\right) \right\} \tag{7}$$

for $i = 1,\dots,k$, for all $\mathbf{v}_h \in \mathbf{V}_h$, and for all $q_h \in Q_h$, where $\alpha_{i,j}^c$ and β_i^c are defined by

$$\alpha_{i,j}^c := \hat{\phi}_j'(\hat{t}_i) + \beta_i^c \hat{\phi}_j'(\hat{t}_0), \quad \beta_i^c := \hat{w}_0 \hat{\psi}_i(\hat{t}_0), \quad i = 1,\dots,k, j = 0,\dots,k,$$

see [9].

In the following, we write (7) as a nonlinear algebraic block system. For simplicity, we restrict ourselves to the two-dimensional case. The three-dimensional case is obtained in a straightforward manner.

Let $\{\phi_i \in Y_h, i = 1,\dots,m_h\}$ be a finite element basis of Y_h and $\xi_{n,1}^j, \xi_{n,2}^j \in \mathbb{R}^{2m_h}$ denote the nodal vectors associated to the components of the finite element function $U_{n,h}^j \in \mathbf{V}_h$ such that

$$U_{n,h}^j(x) = \sum_{l=1}^{2} \left(\sum_{\nu=1}^{m_h} \left(\xi_{n,l}^j\right)_\nu \phi_\nu(x) \right) e^l, \quad x \in \Omega,$$

where $e^1, e^2 \in \mathbb{R}^2$ are the canonical unit vectors. Similarly for the pressure, let $\{\psi_i \in Q_h,\ i = 1,\dots,n_h\}$, denote a finite element basis of Q_h and η_n^j the nodal vector of $P_{n,h}^j \in Q_h$ such that

$$P_{n,h}^j(x) = \sum_{\nu=1}^{m_h} \left(\eta_n^j\right)_\nu \psi_\nu(x), \quad x \in \Omega.$$

Furthermore, the mass matrix $M \in \mathbb{R}^{m_h \times m_h}$, the matrix $A \in \mathbb{R}^{m_h \times m_h}$, the velocity-pressure coupling matrices $B_i \in \mathbb{R}^{n_h \times m_h}$, and the right-hand side vectors $F_{n,i}^j \in \mathbb{R}^{m_h}$, $i = 1,2$, are given by

$$(M)_{s,k} := (\phi_k, \phi_s), \qquad (A)_{s,k} := \nu(\nabla\phi_k, \nabla\phi_s),$$
$$(B_i)_{s,k} := -\left(\psi_s, \nabla\cdot(\phi_k e^i)\right), \qquad (F^j_{n,i})_k := \left(f(t_{n,j}), \phi_k e^i\right), \quad i = 1,2.$$

For a given discrete velocity field $\mathbf{w}_h \in \mathbf{V}_h$ and its nodal vector $\overline{\mathbf{w}} \in \mathbb{R}^{2m_h}$, the matrix representation $N(\overline{\mathbf{w}}) \in \mathbb{R}^{m_h \times m_h}$ of the nonlinear term is defined by

$$\left(N(\overline{\mathbf{w}})\right)_{s,k} := \left(\left(\mathbf{w}\cdot\nabla\right)\phi_k, \phi_s\right). \tag{8}$$

We define the block matrices

$$\mathscr{M} = \begin{bmatrix} M & 0 & 0 \\ 0 & M & 0 \\ 0 & 0 & 0 \end{bmatrix}, \qquad \mathscr{A} = \begin{bmatrix} A+N(\overline{\mathbf{w}}) & 0 & B_1^T \\ 0 & A+N(\overline{\mathbf{w}}) & B_2^T \\ B_1 & B_2 & 0 \end{bmatrix}, \tag{9}$$

and the block vectors

$$F^j_n = \begin{bmatrix} F^j_{n,1} \\ F^j_{n,2} \\ 0 \end{bmatrix}, \qquad \zeta^j_n = \begin{bmatrix} \xi^j_{n,1} \\ \xi^j_{n,2} \\ \eta^j_n \end{bmatrix}. \tag{10}$$

Then, the fully discrete problem (7) on I_n is equivalent to the nonlinear $k \times k$ block system:

Find $\zeta^j_n \in \mathbb{R}^{2m_h+n_h}$, $j = 1,\ldots,k$, such that

$$\sum_{j=0}^{k} \mathscr{M}\zeta^j_n + \frac{\tau_n}{2}\mathscr{A}\zeta^i_n = \frac{\tau_n}{2}\left\{F^i_n + \beta^c_i\left(F^0_n - \mathscr{A}\zeta^0_n\right)\right\}, \quad i = 1,\ldots,k. \tag{11}$$

3.2 The discontinuous Galerkin method

The discontinuous Galerkin (dG) method applied to (4) leads to the following problem in I_n:

Given $\mathbf{u}^-_n$ with $\mathbf{u}^-_1 = \mathbf{u}_{0,h}$, find $\mathbf{u}_{h,\tau}\big|_{I_n} \in \mathbb{P}_k(I_n, \mathbf{V}_h)$ and $p_{h,\tau}\big|_{I_n} \in \mathbb{P}_k(I_n, Q_h)$ such that for all $\psi \in \mathbb{P}_k(I_n)$

$$\int_{I_n} \left[\left(\mathbf{u}'_{h,\tau}, \mathbf{v}_{h,\tau}\right) + A\left(\mathbf{u}_{h,\tau}, (\mathbf{u}_{h,\tau}, p_{h,\tau}), (\mathbf{v}_h, q_h)\right)\right]\psi(t) + \left([\mathbf{u}_{h,\tau}]_n, \mathbf{v}^+_{n-1}\right)\psi(t_{n-1}) = \int_{I_n}\left(\mathbf{f}, \mathbf{v}_{h,\tau}\right)\psi(t)$$

for all $\mathbf{v}_h \in \mathbf{V}_h$ and all $q_h \in Q_h$. Here, the right-sided Gauß-Radau quadrature formula with $(k+1)$ points is applied to evaluate the time integrals numerically. Note that this quadrature rule is exact for polynomials of degree less than or equal to $2k$. Let $\hat{t}_j$ and $\hat{w}_j$, $j = 1,\ldots,k+1$, denote the points and weights for this quadrature formula on $[-1,1]$, respectively.

Since $\mathbf{u}_{h,\tau}$ and $p_{h,\tau}$ restricted to the interval I_n are $\mathbf{V}_h$-valued and Q_h-valued polynomials of degree less than or equal to k , they can be represented as

$$\mathbf{u}_{h,\tau}\big|_{I_n}(t) = \sum_{j=1}^{k+1} U^j_{n,h}\phi^j_{n,h}(t), \qquad p_{h,\tau}\big|_{I_n}(t) = \sum_{j=1}^{k+1} P^j_{n,h}\phi^j_{n,h}(t)$$

with $U^j_{n,h} \in \mathbf{V}_h$ and $P^j_{n,h} \in Q_h$, $j = 1,\ldots,k+1$. Following [2], one obtains the following coupled system of nonlinear equations:

Given $U^0_{n,h} = \mathbf{u}_{0,h}$ for $n = 1$ and $U^0_{n,h} = U^{k+1}_{n-1}$ for $n \geq 2$, find the coefficients $\left(U^j_{n,h}, P^j_{n,h}\right) \in \mathbf{V}_h \times Q_h$, $j = 1,\ldots,k+1$, such that

$$\sum_{j=1}^{k+1} \alpha^d_{i,j}\left(U^j_{n,h}, \mathbf{v}_h\right) + \frac{\tau_n}{2}A\left(U^i_{n,h}, (U^i_{n,h}, P^i_{n,h}), (\mathbf{v}_h, q_h)\right) = \beta_i\left(U^0_{n,h}, \mathbf{v}_h\right) + \frac{\tau_n}{2}\left(\mathbf{f}(t_{n,i}), \mathbf{v}_h\right) \tag{12}$$

for $i = 1,\ldots,k+1$ and for all $(\mathbf{v}_h, q_h) \in (\mathbf{V}_h, Q_h)$ where

$$\alpha_{i,j}^d := \hat{\phi}_j' + \beta_i^d \hat{\phi}_j(-1), \quad \beta_i^d := \frac{1}{\hat{w}_i}\hat{\phi}_i(-1).$$

Similarly as for cGP, problem (12) on I_n results in the $(k+1)\times(k+1)$ nonlinear algebraic block system:

Find $\zeta_n^j \in \mathbb{R}^{2m_h+n_h}$ for $j = 1,\dots,k+1$ such that

$$\sum_{j=1}^{k+1} \alpha_{i,j}^d \mathscr{M}\zeta_n^j + \frac{\tau_n}{2} A\zeta_n^i = \beta_i^d \mathscr{M}\zeta_n^0 + \frac{\tau_n}{2} F_n^i. \tag{13}$$

After solving this system, we enter the next time interval and set the initial value of the time interval I_{n+1} to $\zeta_{n+1}^0 := \zeta_n^{k+1}$.

3.3 Post-processing

In [9], a simple post-processing for systems of ordinary differential equations was presented which was extended to time-dependent convection-diffusion-reaction equations in [10] and to transient Stokes problems in [2]. This simple post-processing allows to construct numerical approximations being in integral-based norms at least one order better than the originally obtained numerical solution provided that the exact solution is sufficiently smooth in time.

We will generalize the idea to the Navier-Stokes equations. Let $\mathbf{u}_{h,\tau}$ and $p_{h,\tau}$ denote the solution of either cGP(k) or dG(k). The post-processed solution $\left(\Pi\mathbf{u}_{h,\tau}, \Pi p_{h,\tau}\right)$ on the time interval I_n is given by

$$(\Pi\mathbf{u}_{h,\tau})(t) = \mathbf{u}_{h,\tau}(t) + g_n\zeta_n(t), \quad (\Pi p_{h,\tau})(t) = p_{h,\tau}(t) + d_n\zeta_n'(t), \qquad t \in I_n,$$

where $g_n \in \mathbf{V}_h$ and $d_n \in Q_h$ are finite element functions and

$$\zeta_n(t) = \frac{\tau_n}{2}\hat{\zeta}(\hat{t}), \quad \hat{t} := T_n^{-1}(t),$$

with T_n from (6). For cGP(k), the polynomial $\hat{\zeta} \in \mathbb{P}_{k+1}$ vanishes in all Gauß-Lobatto points while the polynomial $\hat{\zeta} \in \mathbb{P}_{k+1}$ for dG(k) vanishes in all Gauß-Radau points. In both cases, it is scaled such that $\hat{\zeta}'(1) = 1$. The nodal vectors $\gamma_{n,1} \in \mathbb{R}^{m_h}$, $\gamma_{n,2} \in \mathbb{R}^{m_h}$ of the finite element function $g_n \in \mathbf{V}_h$ and the nodal vector $\delta_n \in \mathbb{R}^{n_h}$ of the finite element function $d_n \in Q_h$ are the solution of the saddle-point problem

$$\begin{bmatrix} M & 0 & B_1^T \\ 0 & M & B_2^T \\ B_1 & B_2 & 0 \end{bmatrix} \begin{bmatrix} \gamma_{n,1} \\ \gamma_{n,2} \\ \delta_n \end{bmatrix} = \begin{bmatrix} F_{n,1}^e \\ F_{n,2}^e \\ 0 \end{bmatrix} - \begin{bmatrix} A+N(\xi_n) & 0 & B_1^T \\ 0 & A+N(\xi_n) & B_2^T \\ B_1 & B_2 & 0 \end{bmatrix} \begin{bmatrix} \xi_{n,1}^e \\ \xi_{n,2}^e \\ \eta_n^e \end{bmatrix} - \begin{bmatrix} M & 0 & 0 \\ 0 & M & 0 \\ 0 & 0 & 0 \end{bmatrix} \begin{bmatrix} \chi_{n,1}^e \\ \chi_{n,2}^e \\ 0 \end{bmatrix} \tag{14}$$

where $\chi_{n,1}^e$, $\chi_{n,2}^e \in \mathbb{R}^{m_h}$ denote the nodal representation of $\mathbf{u}_{h,\tau}'(t_n) \in V_h$ while $\xi_n^e = (\xi_{n,1}^e, \xi_{n,2}^e)^T$ and η_n^e are the nodal vectors for $\mathbf{u}_{h,\tau}(t_n)$ and $p_{h,\tau}$, respectively. The matrices are given in (8) and (9).

It has been shown in [9] for systems of ordinary equations that the post-processed solution $\Pi\mathbf{u}_{h,\tau}(t)$ can be interpreted as the solution of a time stepping scheme with ansatz order $k+1$. The extension to the transient Stokes problems and transient Oseen problems can be found in [2] and [11]. It has been shown numerically that the simple post-processing leads to solutions which show at the discrete time points a super-convergence of order $2k$ (cGP(k)) and $2k+1$ (dG(k)) for both velocity and pressure. Note that the post-processing requires, even for the Navier–Stokes equations, just the solution of a linear saddle point system. The post-processing for the three-dimensional case is obtained in the obvious way.

4 Numerical results

This section is devoted to an example which illustrates accuracy and performance of combinations of inf-sup stable spatial discretizations with higher order variational time discretization schemes. All computations used the finite element code MooNMD [12].

We consider the well-known benchmark problem of the flow around a circle defined in [13]. The geometry and the initial grid (level 0) are given in Fig. 1.

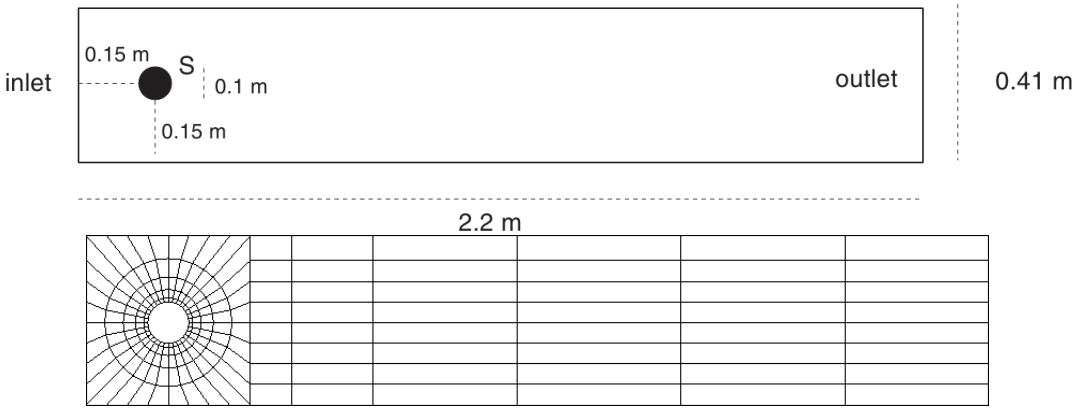

Fig. 1 Domain (top) and initial mesh (bottom) of the test problem.

The Navier-Stokes equations (1) are considered with source term $\mathbf{f} = 0$, viscosity $\nu = 10^{-3}$, and the final time $T = 8$. The inflow and outflow boundary conditions are prescribed by

$$\mathbf{u}(t;0,y) = \mathbf{u}(t;2.2,y) = \frac{1}{0.41^2}\sin\left(\frac{\pi t}{8}\right)\begin{pmatrix}6y(0.41-y)\\0\end{pmatrix}, \qquad 0 \le y \le 0.41,$$

while no-slip conditions are applied on all other boundaries. The diameter of the cylinder is $L = 0.1$ and the mean inflow velocity is $U(t) = \sin(\pi t/8)$ such that $U_{\max} = 1$. The density of the fluid is $\rho = 1$. Hence, the Reynolds number of this flow is $Re = 100$.

Important quantities of interest in this example are the drag coefficient c_d at the circle and the lift coefficient c_l at the circle which are defined by

$$\begin{aligned} c_d(t) &:= \frac{2}{\rho L U_{\max}^2}\int_S \left(\rho\nu\frac{\partial u_{t_S}(t)}{\partial \mathbf{n}}n_y - p(t)n_x\right) dS,\\ c_l(t) &:= -\frac{2}{\rho L U_{\max}^2}\int_S \left(\rho\nu\frac{\partial u_{t_S}(t)}{\partial \mathbf{n}}n_x + p(t)n_y\right) dS, \end{aligned}$$

where $\mathbf{n} = (n_x, n_y)^T$ is the unit normal vector on S directing into Ω, $\mathbf{t}_S = (n_y, -n_x)^T$ the unit tangential vector and $u_{t_S} := \mathbf{u}\cdot\mathbf{t}_S$ the tangential velocity along the circle. Using integration by parts and the weak formulation (4) of the Navier–Stokes equations, we get

$$c_d(t) = -20\big\{(\mathbf{u}_t, \mathbf{v}_d) + \nu(\nabla\mathbf{u}, \nabla\mathbf{v}_d) + \big((\mathbf{u}\cdot\nabla)\mathbf{u}, \mathbf{v}_d\big) - (p, \nabla\cdot\mathbf{v}_d)\big\}$$

for any function $\mathbf{v}_d \in \big(H^1(\Omega)\big)^2$ with $(\mathbf{v}_d)\big|_S = (1,0)^T$ and $\mathbf{v}_d = (0,0)^T$ on all other boundaries. Similarly, the lift coefficient can be obtained by

$$c_l(t) = -20\big\{(\mathbf{u}_t, \mathbf{v}_l) + \nu(\nabla\mathbf{u}, \nabla\mathbf{v}_l) + \big((\mathbf{u}\cdot\nabla)\mathbf{u}, \mathbf{v}_l\big) - (p, \nabla\cdot\mathbf{v}_l)\big\}$$

with any $\mathbf{v}_l \in \big(H^1(\Omega)\big)^2$ as a test function such that $\mathbf{v}_l\big|_S = (0,1)^T$ and $\mathbf{v}_l = (0,0)^T$ on all other boundaries.

The third benchmark parameter is the pressure difference between the front and the back of the circle, given by

$$\Delta p(t) = p(t;0.15,0.2) - p(t;0.25,0.2).$$

The Navier-Stokes equations were discretized in space with the inf-sup stable pairs Q_2/P_1^{disc} and Q_3/P_2^{disc} on quadrilateral meshes. They are obtained from the coarsest mesh (level 0) given in Fig. 1 by regular refinement with boundary adaption to take the curved boundary at the circle into consideration. The computations were performed on mesh level 4. This results in $107,712$ degrees of freedom for the velocity and $39,936$ pressure degrees of freedom for Q_2/P_1^{disc} while there are $241,440$ velocity degrees of freedom and $79,872$ pressure degrees of freedom for Q_3/P_2^{disc}. The temporal discretizations cGP$(k+1)$ and dG(k) lead both to a single $(k+1)\times(k+1)$ block system of nonlinear equations in each time step. The computations were performed with the time step lengths $\tau = 0.02\times 2^{-j}$, $j = 1,\dots,4$. The nonlinearity is resolved by a Picard iteration (fixed point iteration) and the resulting linear systems were solved by a flexible GMRES method [14] where coupled multigrid methods with Vanka-type smoothers were used as preconditioner.

The accuracy is measured with respect to the reference values

$$(t^{\text{ref}}_{d,\max}, c^{\text{ref}}_{d,\max}) = (3.93625, 2.950921575),\ (t^{\text{ref}}_{l,\max}, c^{\text{ref}}_{l,\max}) = (5.693125, 0.47795),\ \Delta p^{\text{ref}}(8) = -0.1116$$

given in [15] where $t^{\text{ref}}_{d,\max}$ and $t^{\text{ref}}_{l,\max}$ denote the times at which drag and lift coefficients achieve their maximal values $c^{\text{ref}}_{d,\max}$ and $c_{l,\max^{\text{ref}}}$, respectively. We compute the error to the reference values with respect to the drag and lift coefficients by the distance formula

$$\text{err}_d = \sqrt{(t^{\text{ref}}_{d,\max} - t_{d,\max})^2 + (c^{\text{ref}}_{d,\max} - c_{d,\max})^2}, \qquad \text{err}_l = \sqrt{(t^{\text{ref}}_{l,\max} - t_{l,\max})^2 + (c^{\text{ref}}_{l,\max} - c_{l,\max})^2},$$

see [16]. The error for the pressure difference will be computed by the simple distance to the reference value.

All numbers which will be presented in the following graphs are based on post-processed velocity and post-processed pressure.

Results for the time stepping schemes cGP(2) and dG(1) in combination with the Q_2/P_1^{disc} finite element pair are plotted in Fig. 2. We observe from the simulations that the behavior concerning the accuracy and efficiency is different for different quantities of interest. For the drag coefficient, the best result for both time discretization methods can be obtained by using the time step length $\tau = 0.00125$. For the lift coefficient, dG(1) needs a smaller time step length than cGP(2), see the left plot in Fig. 2. However, the results for the pressure difference are almost independent of the time step length. Comparing the results for both methods, cGP(2) shows the best combination of efficiency and accuracy.

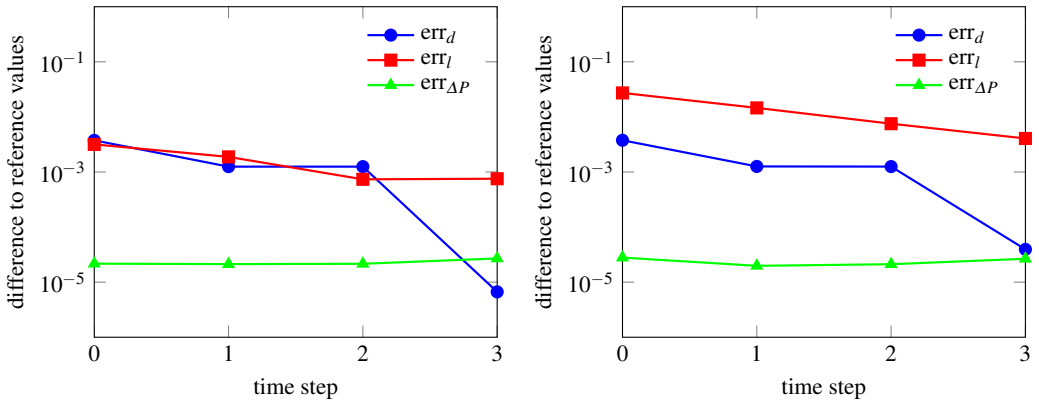

Fig. 2 Difference to the reference values vs the time step lengths for the cGP(2) (left) and dG(1) (right) methods combined with the finite element pair Q_2/P_1^{disc}.

In Figure 3, the differences to reference values for the combination of cGP(3) and dG(2) with the pair Q_3/P_2^{disc} are plotted. Similar conclusions can be made as for the combination of cGP(2) and dG(1) with the pair Q_2/P_1^{disc} if the drag coefficient is of main interest. However, both time discretization methods perform similar for the lift coefficient and pressure difference. Moreover, it is observed that the time error is dominant in the computations of the error of the lift coefficient. This can be seen in Fig. 4 where the difference to the reference time $t^{\text{ref}}_{l,\max}$ and value $c^{\text{ref}}_{l,\max}$ are plotted.

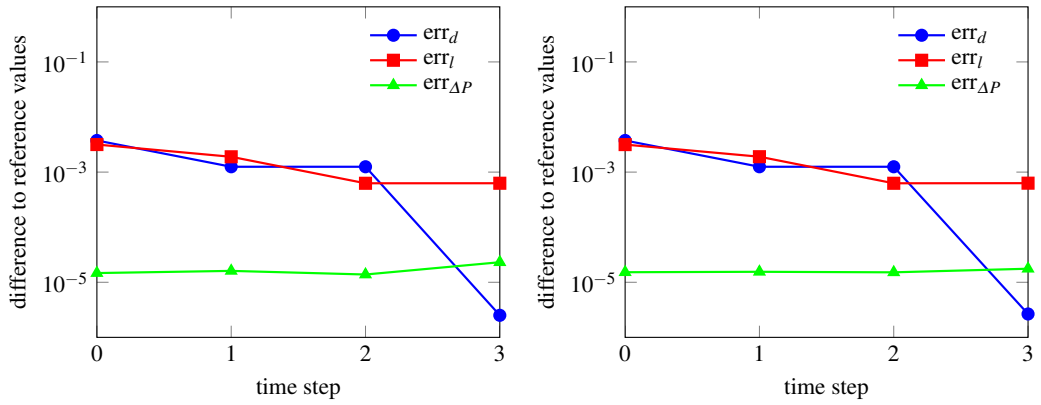

Fig. 3 Difference to the reference values vs the time step lengths for the cGP(3) (left) and dG(2) (right) methods combined with the finite element pair Q_3/P_2^{disc}.

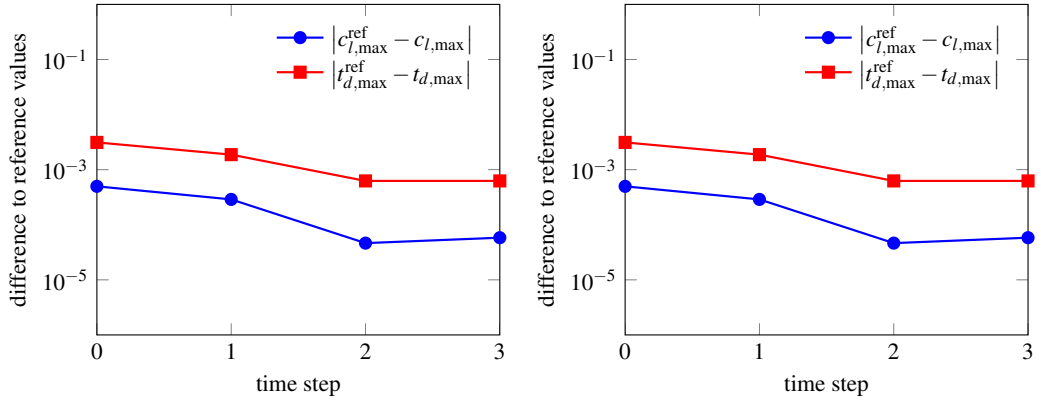

Fig. 4 Difference to the reference maximum time and lift values vs the time step lengths for the cGP(3) (left) and dG(2) (right) methods combined with the finite element pair Q_3/P_2^{disc}.

Fig. 5 shows for the four considered combinations of spatial and temporal discretizations the drag and lift coefficients as well as the pressure difference as a function of time. The corresponding reference curves from [15] are also given in all plots. If the drag coefficient and pressure difference are of concern, all methods produce similarly accurate results. Considering the accuracy of the lift coefficient, the situation is considerably more delicate. The higher order methods cGP(3) and dG(2), both in combination with the higher order pair Q_3/P_2^{disc} as spatial discretization, generate values which are closer to the reference data than the results obtained for cGP(2) and dG(1), both together with Q_2/P_1^{disc} as discretization in space. This can be seen in a zoom of the lift coefficient around $(t_{l,\max}^{\mathrm{ref}}, c_{l,\max}^{\mathrm{ref}})$, shown in the right bottom picture of Fig. 5. The results of the four discretizations suggest that the behavior of the lift coefficient is much more influenced by the spatial discretization than the variational time discretization.

References

1. A. K. Aziz, P. Monk, Continuous finite elements in space and time for the heat equation, Math. Comp. 52 (186) (1989) 255–274.
2. N. Ahmed, S. Becher, G. Matthies, Higher-order discontinuous Galerkin time stepping and local projection stabilization techniques for the transient Stokes problem, Comput. Methods Appl. Mech. Engrg. 313 (1) (2017) 28–52.
3. S. Hussain, F. Schieweck, S. Turek, Higher order Galerkin time discretization for nonstationary incompressible flow, in: Numerical mathematics and advanced applications 2011, Springer, Heidelberg, 2013, pp. 509–517.
4. S. Hussain, F. Schieweck, S. Turek, A note on accurate and efficient higher order Galerkin time stepping schemes for the nonstationary Stokes equations, Open Numer. Methods J. 4 (2012) 35–45.

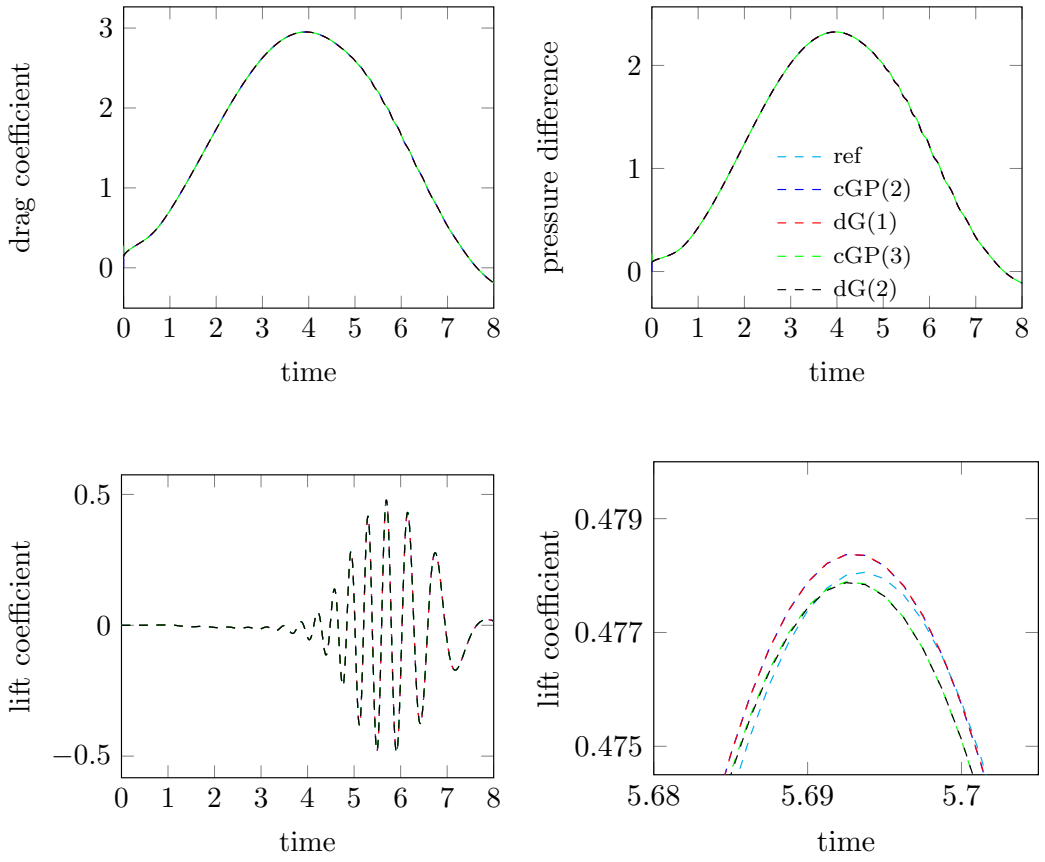

Fig. 5 Evaluation of the drag coefficient (top left), pressure difference (top right), lift coefficient (bottom left), and zoom of the lift coefficient around $(t_{l,\max}^{\text{ref}}, c_{l,\max}^{\text{ref}})$ (bottom right).

5. S. Hussain, F. Schieweck, S. Turek, An efficient and stable finite element solver of higher order in space and time for nonstationary incompressible flow, Internat. J. Numer. Methods Fluids 73 (11) (2013) 927–952.
6. S. Hussain, F. Schieweck, S. Turek, Efficient Newton-multigrid solution techniques for higher order space-time Galerkin discretizations of incompressible flow, Appl. Numer. Math. 83 (2014) 51–71.
7. V. Thomée, Galerkin finite element methods for parabolic problems, 2nd Edition, Vol. 25 of Springer Series in Computational Mathematics, Springer-Verlag, Berlin, 2006.
8. G. Matthies, L. Tobiska, Mass conservation of finite element methods for coupled flow-transport problems, Int. J. Comput. Sci. Math. 1 (2-4) (2007) 293–307.
9. G. Matthies, F. Schieweck, Higher order variational time discretizations for nonlinear systems of ordinary differential equations, Preprint 23/2011, Fakultät für Mathematik, Otto-von-Guericke-Universität Magdeburg (2011).
10. N. Ahmed, G. Matthies, Higher order continuous Galerkin-Petrov time stepping schemes for transient convection-diffusion-reaction equations, ESAIM Math. Model. Numer. Anal. 49 (5) (2015) 1429–1450.
11. N. Ahmed, G. Matthies, Numerical studies of variational-type time-discretization techniques for transient Oseen problem., in: Algoritmy 2012. 19th conference on scientific computing, Vysoké Tatry, Podbanské, Slovakia, September 9–14, 2012. Proceedings of contributed papers and posters., Bratislava: Slovak University of Technology, Faculty of Civil Engineering, Department of Mathematics and Descriptive Geometry, 2012, pp. 404–415.
12. V. John, G. Matthies, MooNMD—a program package based on mapped finite element methods, Comput. Vis. Sci. 6 (2-3) (2004) 163–169.
13. S. Turek, M. Schäfer, Benchmark computations of laminar flow around cylinder, in: E. Hirschel (Ed.), Flow Simulation with High-Performance Computers II, Vol. 52, Vieweg, 1996, pp. 547–566.
14. Y. Saad, A flexible inner-outer preconditioned GMRES algorithm., SIAM J. Sci. Comput. 14 (2) (1993) 461–469.
15. V. John, Reference values for drag and lift of a two-dimensional time dependent flow around a cylinder, International Journal for Numerical Methods in Fluids 44 (2004) 777–788.
16. V. John, J. Rang, Adaptive time step control for the incompressible navierstokes equations, Comput. Methods Appl. Math. 199 (2010) 514–524.